



Performance of CMIP6 models over South America

Anna Carolina Bazzanella¹ · Claudine Dereczynski¹ · Wanderson Luiz-Silva¹ · Pedro Regoto²

Received: 22 May 2023 / Accepted: 23 September 2023 / Published online: 17 October 2023
© The Author(s), under exclusive licence to Springer-Verlag GmbH Germany, part of Springer Nature 2023

Abstract

Assessing the performance of global climate models in the present is essential to attribute confidence to their future projections. This work aims to evaluate the ability of 28 ‘Sixth Phase of the Coupled Models Intercomparison Project’ (CMIP6) models to represent the South American (SA) climate during the reference period (1995–2014). Using the top 7 selected models that best represent the SA climate (CMIP6-SA), it will be possible to obtain better simulations than CMIP6. The made assessment compares the seasonal austral summer and winter climatologies simulated by the CMIP6 models to the Global Precipitation Climatology Project (GPCP) dataset and the European Center for Medium-Range Weather Forecasts Reanalysis 5 (ERA5) Reanalysis. Also, the performance of the 28 models was objectively evaluated through Taylor Diagrams, using their precipitation monthly time series (1980–2014) and temperature monthly time series (1950–2014). The Top7-CMIP6-SA precipitation annual cycle is also evaluated concerning GPCP and the ensemble of all 28 models used in this study. The results show that, at lower levels, most models offer a good performance to represent the South Atlantic and South Pacific Subtropical Anticyclones, the Intertropical Convergence Zone (ICTZ), and the South Atlantic Convergence Zone, except for AWI-ESM-1-1-LR, BCC-ESM1, and IITM-ESM, which do not provide a good representation of these systems. At upper levels, most models overestimate the magnitude of the Subtropical and Polar Jets. Most models can adequately represent the position of the Bolivian High and the Northeast Brazilian Trough, except AWI-ESM-1-1-LR, CAS-ESM2-0, CNRM-ESM2-1, FGOALS-f3-L, GISS-E2-1-G, IITM-ESM, INM-CM5-0, IPSL-CM6A-LR-INCA, MPI-ESM-1-2-HAM e NESM3. Regarding the annual precipitation cycle, the ensemble of the Top7-CMIP6-SA presents a better performance at some AR6 regions compared with the 28 models’ ensemble, especially over the north of SA.

Keywords Climate variability · Climatology · GCM · ESM · Evaluation

1 Introduction

Climate change is already a reality around the globe. Increasing weather and climate extreme events have exposed millions of people to acute food insecurity and reduced water security, with the most significant adverse impacts observed in many locations and communities, including South America (SA; IPCC 2023—IPCC Synthesis Report).

According to Arias et al. (2021)—(Technical Summary from WG1), besides the overall warming in SA, the mean

and extreme precipitation in South-Eastern South America has been increasing since the 1960s (high confidence). Also, there are decreasing trends in mean precipitation and increasing trends in agricultural and ecological drought over Northeastern South America (medium confidence).

Since 1995, the Coupled Model Intercomparison Project (CMIP) has been organizing climate model experiments involving international climate modeling groups. It has led to a better understanding of past, present, and future climate. The CMIP experiments have been the basis for the Intergovernmental Panel on Climate Change (IPCC) Assessment Reports (ARs). The CMIP6 (The Sixth Phase of the CMIP; O’Neill et al. 2016) was used in the Sixth IPCC AR (AR6; IPCC 2021). The studies by Arias et al. (2021), Dias and Reboita (2021), and Ortega et al. (2021) highlight the improvements of the CMIP6 numerical models compared to the previous version (CMIP5; Taylor et al. 2012), such as the precipitation simulation over the SA tropical region.

✉ Anna Carolina Bazzanella
bazzanellaannacarolina@gmail.com

¹ Department of Meteorology, Institute of Geosciences,
Federal University of Rio de Janeiro – UFRJ, Rio de Janeiro,
Brazil

² National Institute for Space Research – INPE,
Cachoeira Paulista, São Paulo, Brazil

Recent studies have found that CMIP6 models can capture several spatial temperatures and precipitation patterns over the continental region; however, the representation of some SA climate features still needs improvements. The precipitation and temperature magnitude simulations still present systematic errors in the continent and adjacent oceans, such as the underestimation of the precipitation associated with the misrepresentation of cloud physics and the temperature underestimation over the central area of South America in the winter (Ortega et al. 2021). The models can also not correctly represent mesoscale phenomena, such as circulation patterns in the eastern Andes (Pabón-Caicedo et al. 2020).

Almazroui et al. (2021) analyzed the performance of a 38 CMIP6 models ensemble on the present climate in SA, comparing the ensembles' precipitation and air temperature simulations with observations. They noted that the ensemble has great difficulty simulating total rainfall over regions with topographic heterogeneity, presenting a dry bias over the northern Amazon. Dias and Reboita (2021) evaluated 46 CMIP6 models in tropical SA and selected the best seven models. Compared to the complete ensemble of 46 models, the authors also observed reduced precipitation and air temperature bias in some SA sectors when using the seven selected models' ensemble. However, so far, there is no knowledge of studies that spatially evaluate the performance of the CMIP6 models individually to verify if they can reproduce the major climatological systems and the atmospheric circulation patterns that modulate the SA climate.

Given the great utility of the CMIP6 models, mainly related to their projections, this study aims to evaluate their performance in representing the present climate (1995–2014) over SA. We expect a good model's simulation in the current climate may confer some reliability on its projections. Thus, this work aims to answer the following two questions: (i) Are all CMIP6 models able to individually reproduce the SA climate? (ii) Which are the best CMIP6 models in the simulation of the SA climate?

2 Methodology

2.1 Observed dataset

Global Precipitation Climatology Project (GPCP; Adler et al. 2003) and the European Centre for Medium-Range Weather Forecast Reanalysis 5 (ECMWF—ERA5; Hersbach et al. 2020) are the two datasets used as references to assess the CMIP6 models performance. GPCP was developed in 1998 by the World Climate Research Program (WRCP) to produce global monthly precipitation data, integrating meteorological stations, remote sensing, and satellite data. The GPCP dataset used in this study covers the period 1980–2014 with a $2.5^\circ \times 2.5^\circ$ spatial resolution.

ERA5 is the fifth generation of global reanalysis produced by ECMWF, after the First Global Experiment of the Global Atmospheric Research Program (FGGE), ERA-15, ERA-40, and ERA-Interim. ERA5 outputs cover the period 1950–2014 with $0.25^\circ \times 0.25^\circ$ horizontal resolution, and it has been widely used to assess the climate models' performance (Kim et al. 2020; Collazo et al. 2022). The variables used in this study are (i) mean sea level pressure (MSLP), (ii) mean air temperature, and (iii) wind data at upper levels of the troposphere (250 hPa).

2.2 CMIP6 models

Since 1995, CMIP has organized climate model experiments involving international climate modeling groups. Those CMIP experiments have been the base of the IPCC ARs. The newer phase of CMIP (CMIP6) consists of some typical experiments, such as the DECK (Diagnostic, Evaluation, and Characterization of Klima), historical simulations (1850–present), and an ensemble Endorsed Model Intercomparison Projects (MIPs).

Table 1 shows the 28 CMIP6 models evaluated in this study. We chose one of each of the 28 institutions participating in CMIP6 DECK. The model's horizontal resolutions vary from 100 to 500 km. The ensemble member used in this study was r1i1p1f1 ('r' for realization, 'i' for initialization, 'p' for physics, and 'f' for forcing), except for HADGEM3-GC31-LL, where we used the first member available (r1i1p1f3).

All models' references are listed in Table AII.10 from Annex II of AR6 Group I (IPCC 2021: Annex II: Models). All CMIP6 data used in this study are available at the Earth System Grid Federation portal.

2.3 Assessment of CMIP6 models

2.3.1 The subjective assessment

The subjective assessment compares the austral summer (DJF) and winter (JJA) temperature and precipitation climatologies simulated by each of the 28 CMIP6 models with the ERA5 and GPCP (in case of precipitation) datasets. The CMIP6 models' outputs, ERA5, and GPCP data are interpolated to a typical 1° of latitude by 1° of longitude grid, using the bilinear interpolation method. At lower levels, we check if the models can represent the Intertropical Convergence Zone (ITCZ) and the South Atlantic Convergence Zone (SACZ) positioning and also the magnitude and positioning of the South Atlantic Subtropical High (SASH) and the South Pacific Subtropical High (SPSH). At upper levels, we check if the Bolivian High (BH) and the Northeastern Brazil (NEB) trough and the position and magnitude of Subtropical Jet (SJ) and Polar Jet (PJ) Streams are well represented. Figure 1 shows

Table 1 Coupled Climate and Earth System models participating in CMIP6 DECK, evaluated in this study, and their respective horizontal resolutions

Model	Institution (country/region)	Horizontal resolution (km)
ACCESS-ESM1-5	Commonwealth Scientific and Industrial Research Organization (CSIRO) (Australia)	140
AWI-ESM-1-1-LR	Alfred Wegener Institute (AWI) (German)	170
BCC-ESM1	Beijing Climate Centre (BCC) (China)	250
CanESM5	CCC Ma Canadian Centre for Climate Modelling and Analysis (Canada)	250
CAS-ESM2-0	Chinese Academy of Meteorological Sciences (CAMS) (China)	100
CESM2	National Center for Atmospheric Research (NCAR) (USA)	100
CMCC-ESM2	Centro Euro-Mediterraneo sui Cambiamenti Climatici (CMCC) (Italy)	100
CNRM-ESM2-1	Centre National de Recherches Météorologiques and CERFACS Centre Européen de Recherche et de Formation Avancée en Calcul Scientifique (CNRM and CERFACS) (France)	140
E3SM-1-1-ECA	National laboratories consortium (E3SM) (USA)	100
EC-EARTH3	EC-Earth consortium (Europe)	80
FGOALS-f3-L	Chinese Academy of Sciences (CAS) (China)	90
FIO-ESM-2-0	First Institute of Oceanography and Pilot National Laboratory for Marine Science and Technology (FIO-QNLM) (China)	100
GFDL-ESM4	National Oceanic and Atmospheric Administration, Geophysical Fluid Dynamics Laboratory (NOAA-GFDL) (USA)	100
GISS-E2-1-G	Goddard Institute for Space Studies (NASA-GISS) (USA)	200
HADGEM3-GC31-LL	Met Office Hadley Centre (MOHC) (United Kingdom)	140
IITM-ESM	Centre for Climate Change Research, Indian Institute of Tropical Meteorology (CCCR-IITM) (India)	170
INM-CM5-0	Institute for Numerical Mathematics (INM) (Russia)	150
IPSL-CM6A-LR-INCA	Institut Pierre-Simon Laplace (IPSL) (France)	160
KACE-1-0-G	National Institute of Meteorological Sciences, Korea Meteorological Administration (NIMS-KMA) (Korea)	140
MCM-UA-1-0	University of Arizona (USA)	260
MIROC6	JAMSTEC, AORI, NIES, R-CCS (MIROC consortium)	250
MPI-ESM1-2-HR	Max Planck Institute for Meteorology (MPI-M) (German)	80
MPI-ESM-1-2-HAM	HAMMOZ-Consortium (German)	170
MRI-ESM-2.0	Meteorological Research Institute (MRI) (Japan)	100
NESM3	Nanjing University of Information Science and Technology (NUIST) (China)	170

Table 1 (continued)

Model	Institution (country/region)	Horizontal resolution (km)
NorCPM1	NorESM Climate Modelling Consortium (NCC) (Norway)	190
SAM0-UNICON	Seoul National University (SNU) (South Korea)	100
TaiESM1.0	Research Center for Environmental Changes (AS-RCEC) (China)	100

these SA climate features and the topography of the study area. After this assessment, we select the best seven models representing the first quartile of the 28 CMIP6 models evaluated, considering their performance in representing the SA climate. The selected ensemble of seven models (Top7-CMIP6-SA) is compared with the 28 models (28-CMIP6) by analyzing the annual precipitation and air temperature cycles.

The bias of the temperature and precipitation is given by Eq. 1:

$$\text{bias} = \frac{1}{n} \sum_{i=1}^n \overline{\text{model}_i} - \overline{\text{obs}_i} \quad (1)$$

where model_i and obs_i are the simulated and observed data, respectively, in the present period (1995–2014), the bar indicates the seasonal average (DJF and JJA) and n is the number of years (20).

2.3.2 The objective assessment

The objective assessment compares the times series of mean air temperature (1950–2014) and monthly total precipitation (1980–2014) from each of the 28 CMIP6 models with observations. Taylor Diagrams (Taylor 2001) present statistical metrics for each one of the seven regions included in the IPCC AR6: Northwestern South America (NWS), Northern South America (NSA), Northeastern South America (NES), South American Monsoon (SAM), South-Western South America (SWS), South-Eastern South America (SES), and Southern South America (SSA). The Taylor Diagram provides a statistical summary of how well the simulations can reproduce the observations in terms of spatial correlation (CORR), root mean square error (RMSE), and the ratio between the variances (or standard deviations—SD). The statistical metrics displayed in the Taylor diagram are given

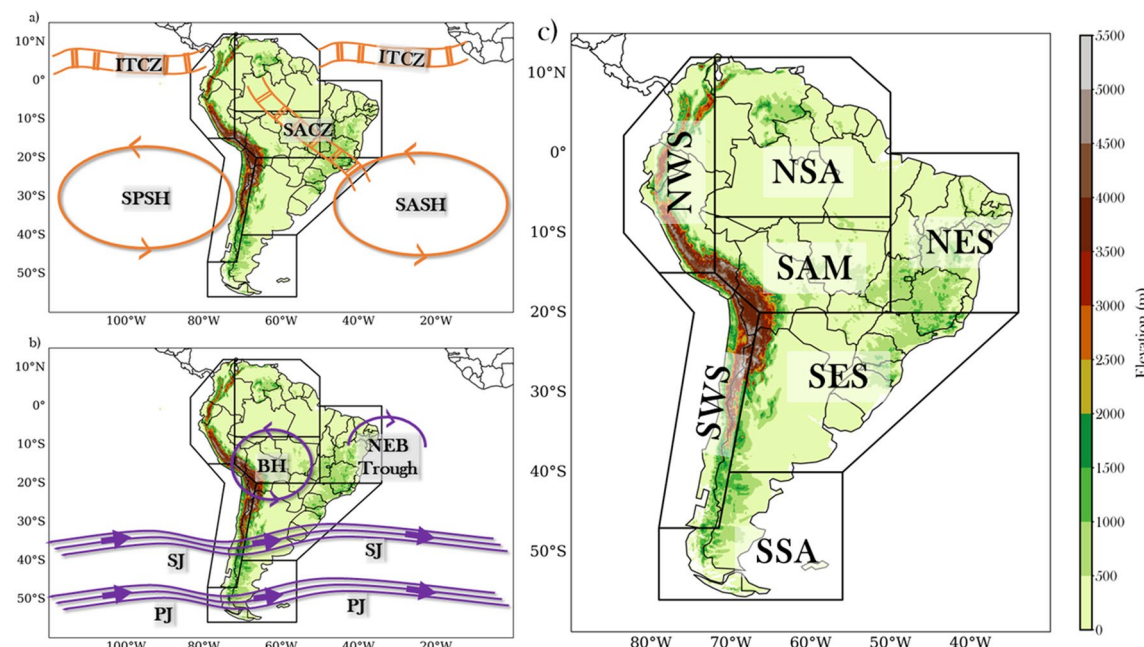


Fig. 1 SA main climate features evaluated in this study at upper (a) and lower (b) levels. c shows the topography (shaded) and the limits of the 7 assessed regions. See the text for the meanings of the acronyms

as follows. SD of the de model and SD of the observed data-set is expressed by Eqs. 2 and 3, respectively:

$$SD_{model} = \sqrt{\frac{\sum_{i=1}^n (model_i - \overline{model})^2}{n}} \quad (2)$$

and

$$SD_{obs} = \sqrt{\frac{\sum_{i=1}^n (obs_i - \overline{obs})^2}{n}} \quad (3)$$

where model_n and obs_n are, respectively, the simulated data and observation in the study period, the bar indicates the time average of these data and n is the number of months in this period (420 months for precipitation and 780 months for temperature).

CORR is expressed as a function of the model_n, obs_n and the SD values (σ_{model} and σ_{obs}), given by Eq. 4:

$$\text{CORR} = \frac{\frac{1}{N} \sum_{n=1}^N (\text{model}_n - \overline{\text{model}})(\text{obs}_n - \overline{\text{obs}})}{\text{SD}_{\text{model}} \text{SD}_{\text{obs}}} \quad (4)$$

CORR values classification is according to the thresholds Mukaka & Moulton (2016) proposed.

Finally, the RMSE in the diagram is expressed as a relation between the CORR and the SD values, following the cosines law as expressed by Eq. 5:

$$\text{RMSE} = \sqrt{\text{SD}_{\text{model}}^2 + \text{SD}_{\text{obs}}^2 - 2\text{SD}_{\text{model}}\text{SD}_{\text{obs}}\text{CORR} + (\overline{\text{model}} - \overline{\text{obs}})^2} \quad (5)$$

3 Results and discussion

3.1 Subjective assessment

In this section, CMIP6 models are evaluated considering their ability to represent SA climatological systems in the present climate (1995–2014) during the austral summer (DJF) and winter (JJA).

3.1.1 Precipitation

Figure 2 shows the 28 CMIP6 models' simulations and the observed climatology for precipitation and MSLP during austral summer. Figure 3 presents the 28 CMIP6 models' spatial bias for precipitation during austral summer. As shown in Fig. 2, most of the models simulate the double-ITCZ over the Pacific and Atlantic Oceans, except MCM-UA-1-0, MPI-ESM-1-2-HAM, NESM3, and SAM0-UNICON, which simulate ITCZ as a single band. In general, models also simulate a southward displacement of the ITCZ compared to its climatological location. Figure 3 shows this aspect, where negative biases reach 120 mm and occur between the equator and 10°N in both oceans. In addition,

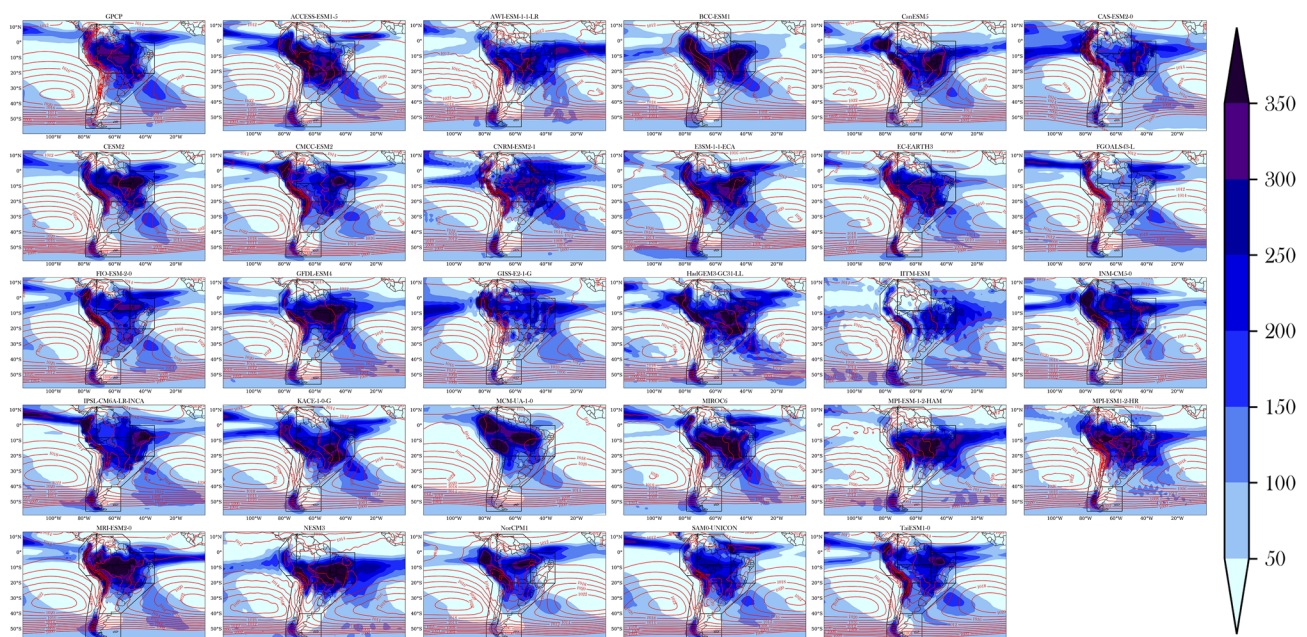


Fig. 2 Austral summer (DJF) climatologies (1995–2014) of precipitation (mm/month) and MSLP (isobars at each 2 hPa) observed (GPCP) and simulated by 28 CMIP6 models

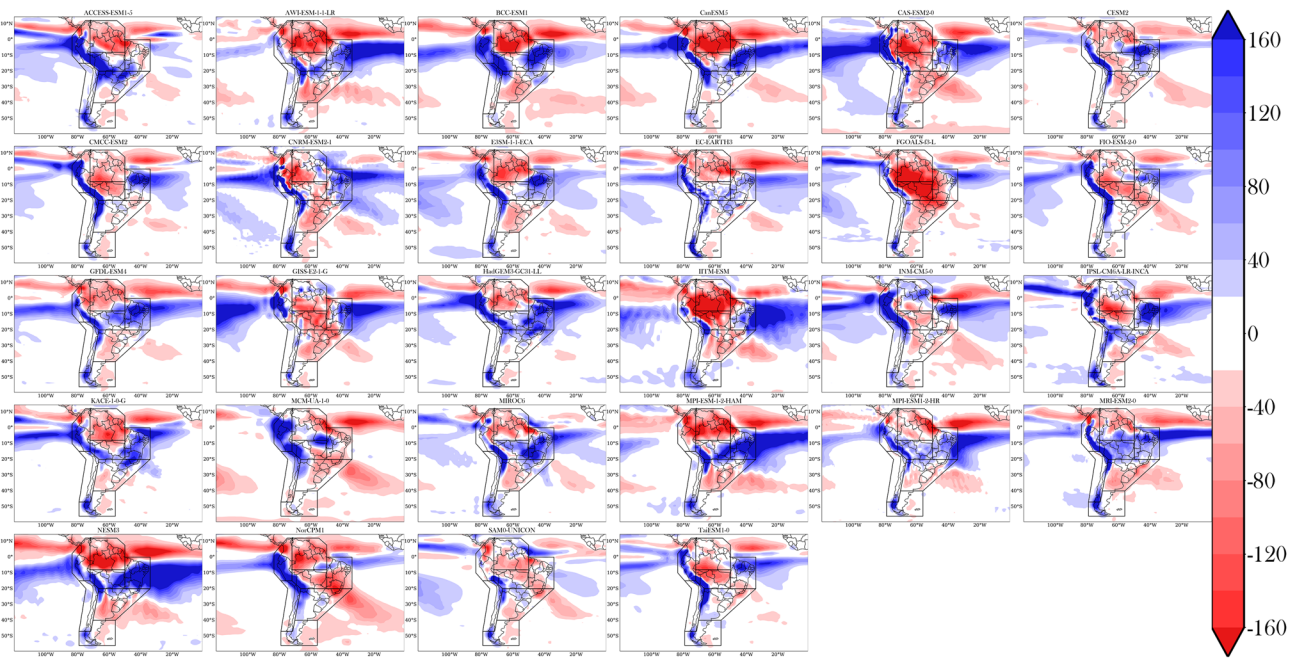


Fig. 3 Austral summer (DJF) precipitation bias (mm) in the period 1995–2014 for the 28 CMIP6 models

associated with the ITCZ southward displacement, precipitation over NES is overestimated in most models.

For this reason, we observe positive bias (up to 100 mm in some models) over NES, except in ACCESS-ESM1-5, MCM-UA-1-0, and SAM0-UNICON models, where the southward displacement of the ITCZ over the Atlantic is not seen. Most models cannot capture the heavy rainfall over the SACZ region, showing a negative bias in NSA and a positive bias in SAM (see Fig. 3). Monteverde et al. (2022) also noted rainfall underestimation over Amazon in some CMIP6 models' simulations, probably associated with their difficulties in reproducing the humidity production linked to local convergence. The SACZ climatological NW–SE orientation is not well represented by AWI-ESM-1-1-LR, BCC-ESM1, GISS-E2-1-G, IITM-ESM, MPI-ESM1-2-HR and CESM3 models (see Fig. 2).

Most models perform well during austral winter (JJA; Figure S1) to simulate ITCZ. ITCZ is displaced to the north this season, relative to its austral summer position. However, some models present a weakened or broken ITCZ band over the continent between the Pacific and Atlantic oceans (Figure S2). For this reason, precipitation is reduced over NSA and in part of NWS (negative bias in Figure S2), especially at AWI-ESM-1-1-LR, BCC-ESM1, FGOALS-f3-L, GFDL-ESM4, IITM-ESM, and MCM-UA-1-0 models. For summer, the ITCZ model's simulation shows a southward displacement compared with its climatological position, which causes an increase (a decrease) of precipitation over the south (north). The local precipitation that occurred over

the NES east coast, especially those associated with easterly wave disturbance, is not well simulated by global models. In some models, the precipitation over NES east coast occurs for another reason: ITCZ incorrect southward displacement (ex: E3SM-1-1-ECA, HadGEM3-GC31-LL, and SAM0-UNICON) or because of the double-ITCZ formation over Atlantic (ex: INM-CM5-0).

3.1.2 MSLP

Figure 2 also shows isobars. The models evaluated present a satisfactory performance to simulate the intensity and positioning of the SPSH during austral summer, except five of them: GISS-E2-1-G, INM-CM5-0, MIROC6, and NESM3, which underestimated the magnitude of its center around 2–4 hPa (Figure not shown). All models show a good performance in simulating the SASH location. Most models correctly simulate the SASH intensity (1020 hPa), but some show positive or negative biases, around 2 hPa. In some models, with SASH inside the continent, precipitation is underestimated because of the predominant atmospheric pressure high values, especially over NES, SAM, and SES, as verified in the FGOALS-f3-L model. On the other hand, in models where SASH is displaced eastward, precipitation is overestimated over NES and SAM, for example, in NESM3.

During austral winter (Figure S1), only some models can simulate the correct magnitude of the SPSH (1020 hPa) and

SASH (1024 hPa) center, while in other models, the error fluctuates around ± 2 hPa. The SPSH positioning and the SASH influence on the continent during winter are crucial characteristics of the SA climate well captured by CMIP6 models.

3.1.3 Mean air temperature

Figure 4 shows the mean air temperature bias during austral summer (DJF), calculated between the 28 CMIP6 models and GPCP. In some models, areas that show precipitation underestimation (overestimation) also present an increase (decrease) in air temperature. This relationship is more evident over NES, a region where most models show a cold bias (Fig. 4), which may be caused by excess simulated precipitation, as seen in Fig. 3. The opposite can be verified over NSA, where the hot bias could be associated with precipitation underestimation. This pattern between these two variables may result from the relationship between model cloudiness and incoming shortwave radiation. The warm bias may also result from errors in the hydrological cycle modeling from the reduced evapotranspiration due to the reduced precipitation. Also, models primarily show a warm bias over SES, especially in northern Argentina. These may be associated with the same difficulty found by Zazulie et al. (2017) in simulating the regional climate of the subtropical central Andes using CMIP5 models. This warm bias can partially be explained by the models' misrepresentation of the steep topography, which results in an underestimation of

altitude over the region. However, these biases still need to be further investigated.

During winter (Figure S3), most models underestimate the temperature over NES, and some also overestimate the temperature over NSA. This warm bias over NSA can be linked to the simulated precipitation deficit, considering the models' difficulty in capturing the ITCZ influence over the SA north region.

3.1.4 Upper-level circulation

Figure 5 shows the 250 hPa wind climatology for austral summer for OBS and the 28 CMIP6 models. Ten models are not able to represent correctly the NEB trough and the BH: AWI-ESM-1-1-LR, CAS-ESM2-0, CNRM-ESM2-1, FGOALS-f3-L, GISS-E2-1-G, IITM-ESM, INM-CM5-0, IPSL-CM6A-LR-INCA, MPI-ESM1-2-HAM and NESM3. Some models represent the NEB trough with an eastward displacement close to 5° of longitude. It can be linked to the BH circulation presenting a large amplitude compared to OBS since both (NEB trough and BH) have an evident interaction due to thermodynamic responses. Furthermore, the BH simulated magnitude seems lower than observed due to the underestimated precipitation over the Amazon, decreasing the latent heat inside the troposphere.

During the austral winter (Figure S4), half of the models overestimate the jet stream's magnitude and displace it 5° of latitude northward. This difficulty in simulating the jet streams can cause a wrong representation of the transient

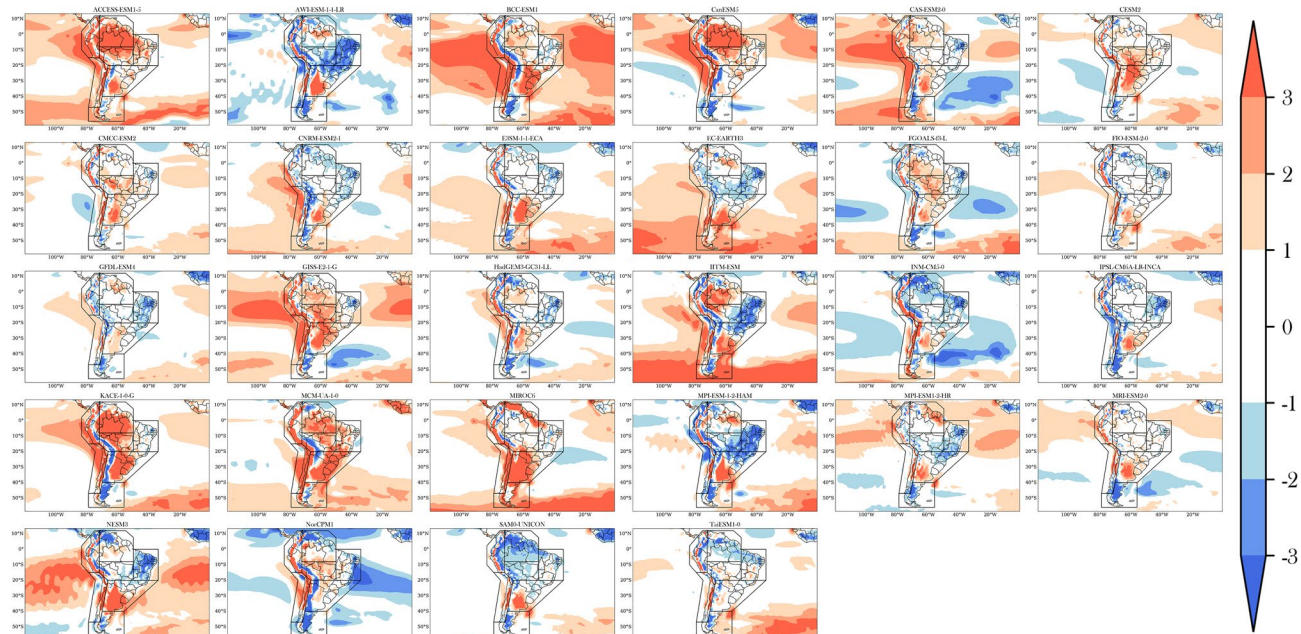


Fig. 4 Austral summer (DJF) mean air temperature bias ($^{\circ}\text{C}$) considering the period 1995–2014

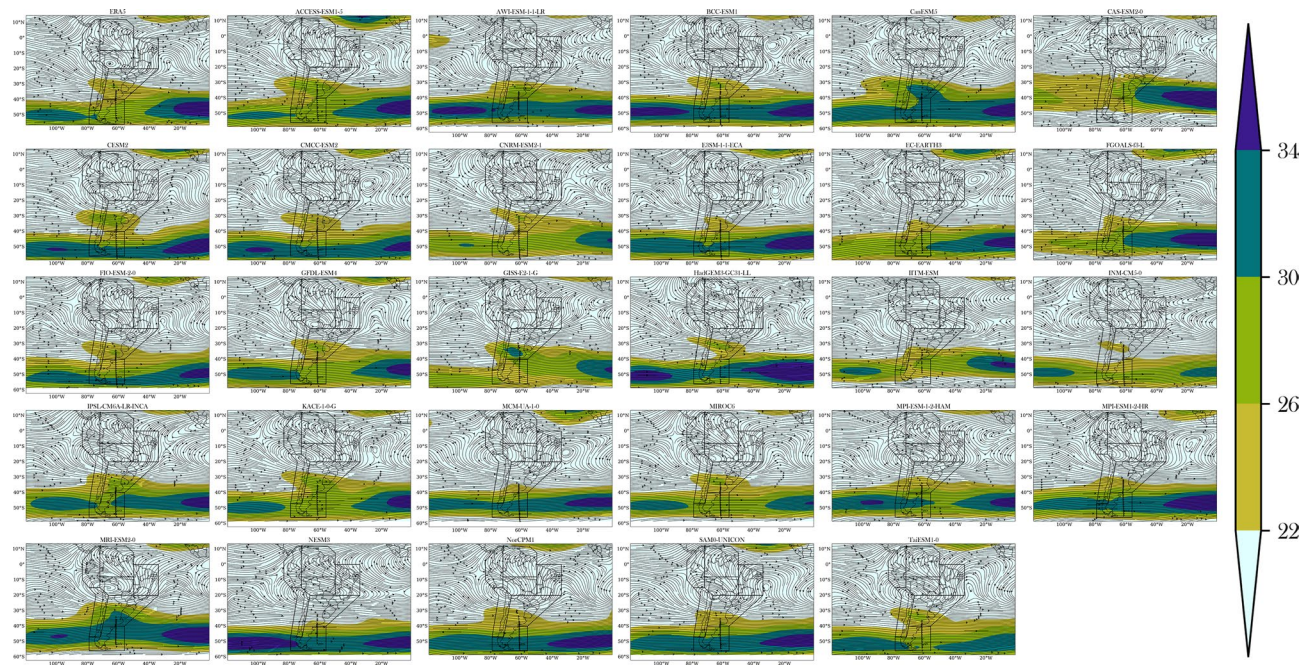


Fig. 5 Austral summer (DJF) climatologies (1995–2014) of streamlines and wind magnitude (m/s) at upper levels (250 hPa) for ERA5 and 28 CMIP6 models

systems paths, also modifying its frequency and magnitude over SA and the Atlantic Ocean.

3.1.5 Summary of subjective analysis

All models present a better performance to simulate the precipitation during austral winter, which is the drought season for most of the SA continent, compared to the rainfall season (austral summer), as observed in Ortega et al. (2021). Models' performance is summarized in Table 2, considering the main SA climate features. During austral summer, all models show a double-ITCZ pattern, which is very common in climate global models, linked to the inadequate representation of the ocean–atmosphere coupling, especially over the Tropical Pacific Ocean (Adam et al. 2017 and Ortega et al. 2021). Tian and Dong (2020) highlighted the slight improvement related to the double-ITCZ from CMIP3 until CMIP6, besides the advances in spatial and vertical resolutions and model parametrizations. During austral winter, models show an outstanding performance to simulate ITCZ over the Pacific. Over the Atlantic, models represent ITCZ positioning well; however, they tend to underestimate the precipitation band. Models also show satisfactory performance in simulating spatial patterns of surface variables, such as mean air temperature and MSLP, correctly simulating the positioning of SASH and SPSH during summer and winter. The deficiency of some models in representing the position and intensity of the upper-level jet stream is worth

mentioning, which can directly influence the bias of precipitation and air temperature on SSA, SES, and SWS.

According to the subjective assessment shown in Sect. 3.1, we selected seven models with the best performance over SA (Top7-CMIP6-SA): ACCESS-ESM1-5, CMCC-ESM2, EC-EARTH3, KACE-1-0-G, MIROC6, MRI-ESM2-0, and TaiESM1-0. Concerning models' configurations with better performance, only two (EC-EARTH3 e TaiESM1-0) of the seven models selected do not have the atmospheric chemical component. Among the seven models, only three (EC-EARTH3, KACE-1-0-G e MIROC6) do not include the carbon cycle in their simulations. In all models, aerosols are computed from emissions.

The Top7-CMIP6-SA ensemble is then compared to the 28-CMIP6 ensemble for their ability to represent the precipitation climatologies for austral summer (Fig. 6) and winter (Figure S5) through the analysis of precipitation bias. In addition, the precipitation and mean air temperature annual cycles (Fig. 7 and Figure S6, respectively) were also evaluated for both ensembles for the seven IPCC AR6 regions, considering the 1950–2014 (65 years) period for temperature and 1980–2014 (35 years) period for precipitation. The main goal of this step is to verify if there is any improvement using the Top7-CMIP6-SA ensemble instead of the 28-CMIP6 ensemble.

Figure 6 shows no significant difference between both ensembles, except over the south extreme of NSA, where Top7-CMIP6-SA performs better than the 28-CMIP6. Still, during the austral summer, the Top7-CMIP6-SA ensemble

Table 2 Summary of the models' performance considering the main SA climate features simulated by models evaluated in the subjective assessment

CMIP6 models	SACZ	ITCZ	SASH	SPSH	BH	NEB trough	SJ	PJ
ACCESS-ESM1-5	↔	↑	↑	↑	↑	↑	↑	↔
AWI-ESM-1-1-LR	↓	↓	↓	↑	↔	↓	↓	↓
BCC-ESM1	↓	↓	↑	↓	↑	↑	↔	↑
CanESM5	↔	↔	↑	↑	↑	↔	↔	↓
CAS-ESM2-0	↓	↔	↓	↓	↓	↓	↓	↓
CESM2	↑	↔	↑	↑	↑	↑	↑	↓
CMCC-ESM2	↑	↑	↑	↑	↑	↑	↑	↔
CNRM-ESM2-1	↑	↔	↑	↑	↓	↓	↑	↑
E3SM-1-1-ECA	↔	↑	↑	↑	↑	↑	↑	↔
EC-EARTH3	↑	↑	↑	↑	↑	↑	↑	↑
FGOALS-f3-L	↓	↑	↔	↑	↓	↓	↓	↑
FIO-ESM-2-0	↑	↑	↑	↑	↑	↑	↑	↔
GFDL-ESM4	↔	↔	↑	↑	↑	↑	↑	↔
GISS-E2-1-G	↓	↓	↑	↓	↓	↓	↓	↔
HADGEM3-GC31-LL	↔	↓	↑	↑	↔	↑	↔	↓
IITM-ESM	↓	↓	↑	↓	↓	↓	↓	↓
INM-CM5-0	↓	↓	↑	↑	↓	↓	↓	↓
IPSL-CM6A-LR-INCA	↓	↔	↑	↑	↓	↓	↔	↓
KACE-1-0-G	↔	↑	↑	↑	↑	↑	↑	↑
MCM-UA-1-0	↓	↓	↑	↓	↓	↑	↔	↔
MIROC6	↑	↑	↔	↑	↑	↑	↑	↔
MPI-ESM1-2-HR	↔	↓	↑	↑	↑	↑	↔	↑
MPI-ESM1-2-HAM	↓	↓	↓	↑	↓	↓	↓	↓
MRI-ESM-2.0	↑	↑	↑	↑	↑	↑	↔	↔
NESM3	↓	↓	↓	↑	↓	↓	↓	↓
NorCPM1	↔	↑	↓	↑	↔	↑	↑	↑
SAM0-UNICON	↔	↑	↑	↑	↑	↑	↑	↑
TaiESM1.0	↔	↑	↑	↑	↑	↑	↑	↑

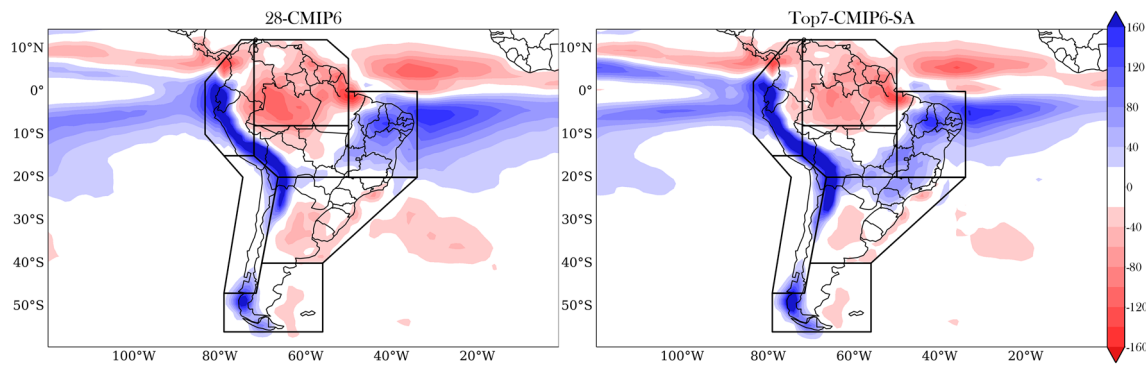


Fig. 6 Precipitation bias (mm) considering the period 1995–2014 for austral summer (DJF) relative to the 28-CMIP6 and Top7-CMIP6-SA ensembles

manages to smoothly reduce the negative biases of the accumulated rainfall over NSA and SES. The situation changes in austral winter (Figure S5), and the Top7-CMIP6-SA exhibits

the best performance in most parts of continental regions, especially over NSA. Over SWS and NWS, precipitation biases are smaller in the 28-CMIP6 ensemble.

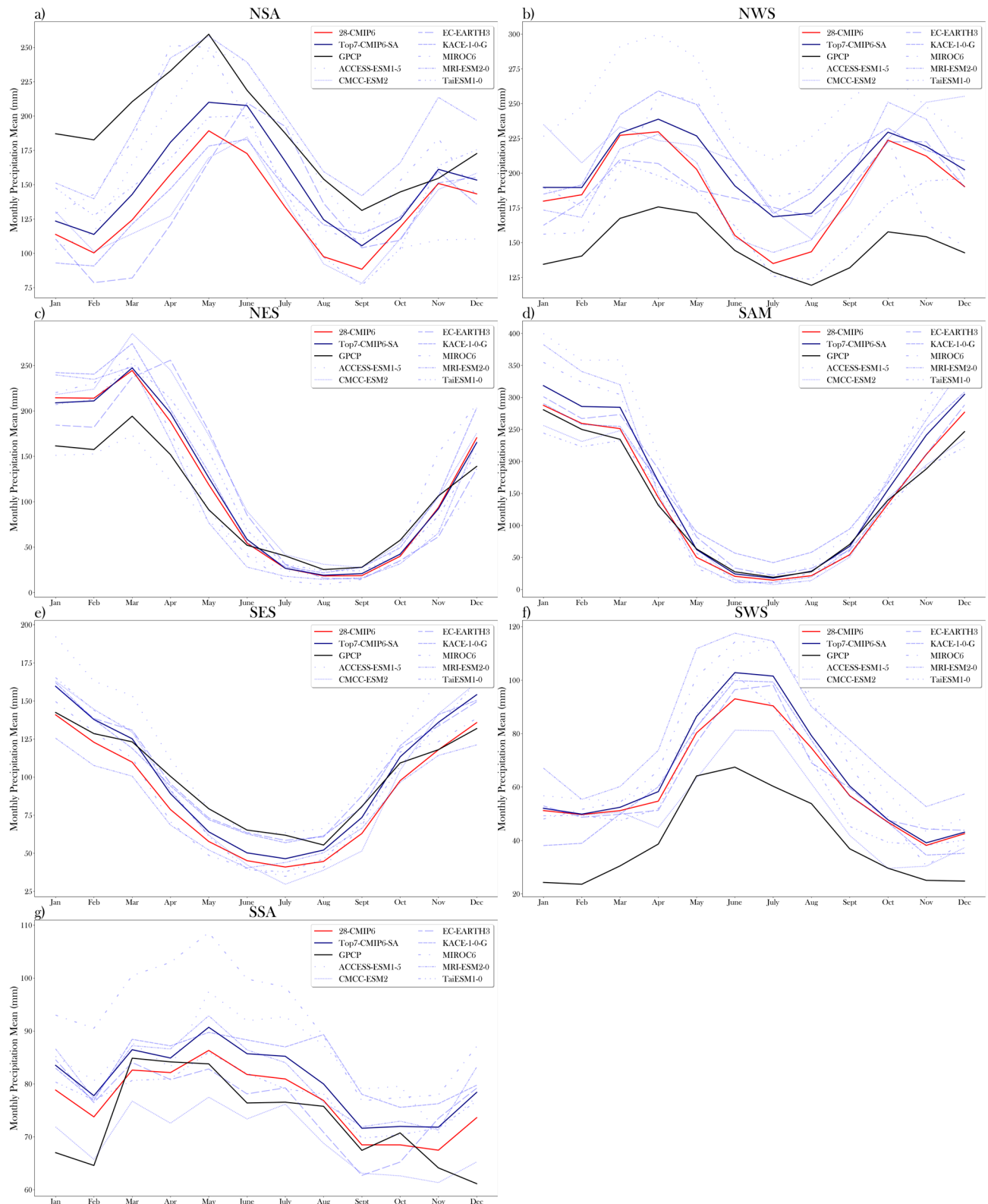


Fig. 7 Precipitation annual cycle for observation (GPCP—black line), the ensembles 28-CMIP6 (red line) and Top7-CMIP6-SA (dark blue line). The diagram also shows the seven models included in Top7-

CMIP6-SA in blue lines. The annual cycle was computed using the period 1980–2014 for the seven AR6 regions

In Fig. 7, the annual cycles are well represented by most of the regions for both ensembles, with precipitation maximums and minimums occurring in phase with observation. However, the amount of precipitation needs to be overestimated (underestimated) by both ensembles over NWS, NES, SAM, SWS, and SSA (NSA and SES). These positive biases over SWS and SSA are likely associated with the models' difficulty in capturing the influence of Andes orography in the regional precipitation regime. In these regions, the westerly winds in the southern SPSH reach the Andes Mountains, forced to ascend, and the flow is adiabatically cooled and favors precipitation (Reboita et al. 2010). Topography also influences precipitation over SAM, which is still challenging for CMIP6 models. During the wet season, there is substantial convective activity due to the orographic effect of humid air upward from the Amazon basin in the eastern sector of the Andes (Garreaud and Wallace 1997). Over NWS and NES, there is a relationship between the excessive precipitation and the southward displacement of the ITCZ. SA monsoon influences precipitation over NSA, which is not well simulated by most models and may be due to the reason for these negative biases. Also, the study of Ridder et al. 2021 shows that CMIP6 models cannot simulate tropical convection because of the need for more spatial resolution to resolve these synoptic-scale phenomena satisfactorily. Ortega et al. (2021) also highlight that the precipitation patterns are not well simulated during the wet season for the Andes hotspot, but these biases are reduced in CMIP6 models.

The annual cycles are well represented regarding the mean air temperature (Figure S6), although there is overestimation and underestimation over most parts of the region. In the NSA, NES, and SAM, pronounced cycles are simulated in both ensembles, with lower (higher) temperatures in winter (summer). Over NSA and NES, temperature biases seem related to precipitation biases. However, this relationship is only evident in some models, as observed in the spatial temperature bias (Fig. 4 and Figure S3), since the misrepresentation can also be related to errors in other processes, such as heat advection, surface interactions, and parameterizations.

These results show that the performance of the ensembles (Top7-CMIP6-SA and 28-CMIP6) depends on the region analyzed. The improvements found in the Top7-CMIP6-SA ensemble compared to the 28-CMIP6 ensemble are more evident in regions where models present the lowest skill for precipitation, as NSA and NWS, and NSA and NES, for temperature. Furthermore, the Top7-CMIP6-SA ensemble presents the same problems seen at the 28-CMIP6 ensemble in the precipitation annual cycle, exhibiting a gap in the months where the variable's maximum and minimum values are observed. Although there are discrepancies in the amount of precipitation, the beginning and the ending of

the rainfall season are relatively well captured by the Top7-CMIP6-SA models simulations.

Over NSA and NES, temperature biases seem related to precipitation biases. However, this relationship is only evident in some models, as observed in the spatial temperature bias (Fig. 4 and Figure S3), since the misrepresentation can also be related to errors in other processes, such as heat advection, surface interactions, and parameterizations. The difficulty in selecting a group of models able to represent the SA climate occurs due to its extensive climatic diversity. Then, the models' selection must be based on the region, variable, and period of the year of interest.

3.2 Objective assessment

In this section, CMIP6 models are evaluated regarding their ability to represent the monthly total precipitation and the monthly mean air temperature, considering the period 1950–2014 (65 years) for temperature and 1980–2014 (35 years) for rainfall. For this objective analysis, we use Taylor Diagrams for both variables and each of the seven AR6 regions shown in Fig. 1. Taylor diagrams constructed with the monthly total precipitation dataset (in mm/month) are shown in Fig. 8. The mean air temperature in Taylor's diagrams is presented in additional material (see Figure S7).

3.3 NSA

In NSA (Fig. 8a), GPCP presents an SD value of 45.5 mm/month, while most models show SD varying between 20 and 70 mm/month. The models' RMSE values are lower than the observed SD, ranging between 30 and 60 mm/month, except for MCM-UA-1-0 and NESM3 models, which present very high RMSE values. Most models show a weak to moderate CORR, varying between –0.1 and 0.7, but mostly around 0.5. Amazon's climate is highly influenced by tropical ocean and interannual oscillations, like El Niño Southern Oscillation (ENSO). Joetzjer et al. (2013) show that difficulties in modeling this phenomenon influence the precipitation over NSA.

About the mean air temperature (Figure S7 a), the models' RMSE values are very high ($0.7 \leq \text{RMSE} < 3.0$) when compared to observation SD, which is 0.7 °C. The CORR values are low, oscillating between 0.3 and 0.7.

3.4 NWS

The NWS (Fig. 8b) is another region in which models show poor performance in the spatial representation of the precipitation. About the RMSE, 24 models present values between 25 and 50 mm/month, close to the observed SD (26.5 mm/month). CORR values are weak for most models, varying between 0.2 and 0.5.

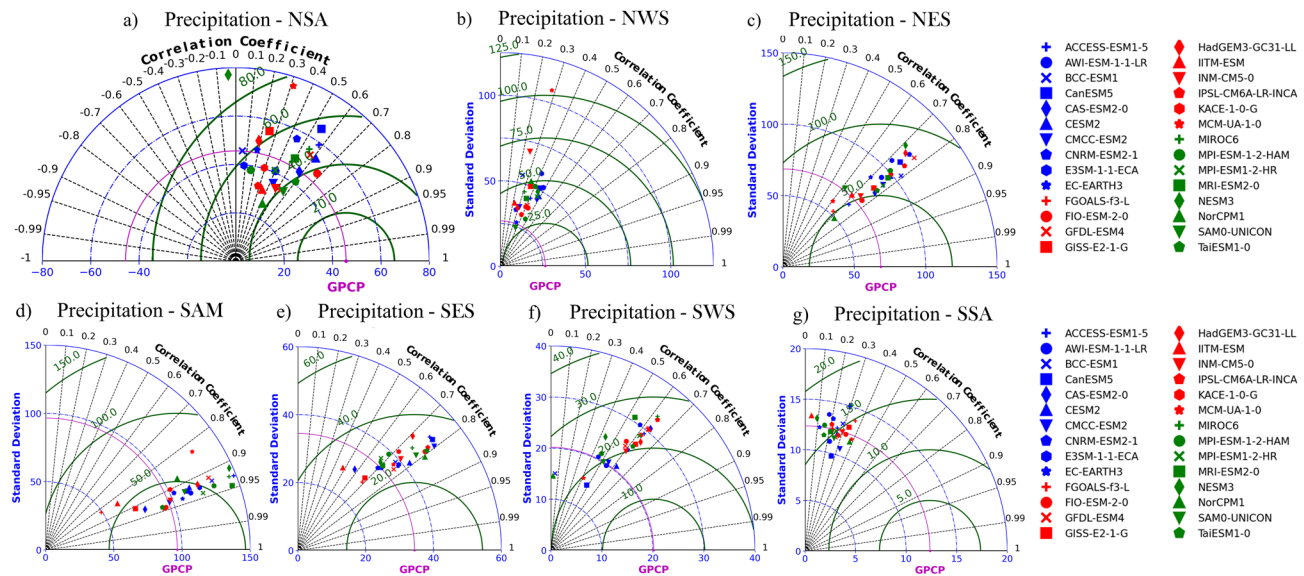


Fig. 8 Taylor diagrams for the seven SA AR6 regions, computed using precipitation monthly time series (1980–2014) of the 28 CMIP6 models and GPCP. The standard deviation values (SDs) in mm/month are in the horizontal and vertical axis, also represented by

the blue dashed line. The pink solid line represents the standard deviation of observation (GPCP). The radial black dashed line represents the coefficient values of spatial correlation (CORR), and finally, semi-circles formed by green solid lines are the RMSE values (mm/month)

For temperature (Figure S7 b), models also show high RMSE values ($\text{RMSE} > 3.0 \text{ }^{\circ}\text{C}/\text{month}$) compared to ERA5 SD, which is $0.9 \text{ }^{\circ}\text{C}/\text{month}$ in this region. However, most models can simulate the temperature annual SD, as it is a region with slight seasonal temperature variations. The significant discrepancy between the models occurs in the spatial correlation since some models present a very weak correlation and others a strong one.

3.5 NES

In NES (Fig. 8c), most of the models show a strong correlation for precipitation ($0.7 \leq \text{CORR} < 0.9$). The observed SD is 6.3 mm/month , exhibiting values between 49 and 121 mm/month . The model NESM3 shows an SD value close to double the observation ($\text{SD} = 121 \text{ mm/month}$) and a high value of RMSE (96.6 mm/month), although a strong correlation (0.7). High values of SD could be associated with the difficulty of some models in representing some of the Atlantic Ocean variability modes (Alves et al. 2016).

There is a similar pattern over NSA about the mean air temperature (Figure S7c): only some models show an SD value close to observation ($0.8 \text{ }^{\circ}\text{C}/\text{month}$). Most of the models represent the temperature spatial distribution well, as 21 models show strong values of CORR ($\text{CORR} \geq 0.7$). Mostly RMSE models' values are also negligible compared with ERA5's SD.

3.6 SAM

Among all the seven regions evaluated, SAM (Fig. 8d) is the region in which models show the better performance in the simulation of the precipitation: $0.8 \leq \text{CORR} < 0.95$, $\text{RMSE} \leq 70 \text{ mm/month}$ (except MCM-UA-1-0) and half of the models (14) show values of SD close to observation ($90 \leq \text{SD} \leq 120 \text{ mm/month}$). SAM region presents a rainfall seasonal cycle well defined as a typical characteristic of tropical climate, which can be associated with the excellent performance of models in terms of spatial correlation.

Regarding the air temperature over SAM (Figure S7 d), the models' RMSE is not so high as the observed SD ($1.2 \text{ }^{\circ}\text{C}/\text{month}$). CORR varies between 0.5 and 0.75 . Most models represent the observed SD value well, suggesting a good performance in simulating the monthly air temperature variation.

3.7 SES

Over SES (Fig. 8e), most of the models show a strong correlation ($0.7 \leq \text{CORR} \leq 0.8$) to simulate the precipitation. Only two models show a moderate correlation: CAS-ESM2-0 ($\text{CORR} = 0.6$) and IITM-ESM ($\text{CORR} = 0.5$). The Observed SD is 34.4 mm/month , and SES is the second region in which most models perform well in representing SD rainfall ($29 \leq \text{DP} \leq 50 \text{ mm/month}$). Models' RMSE values are lower than GPCPs' SD ($20 < \text{RMSE} < 40 \text{ mm/month}$).

Regarding the air temperature (Figure S7 e), SES is one of the three regions where models show a good performance since the correlation values are high ($\text{CORR} \geq 0.9$ —very strong). The models' RMSE is also tiny compared with the SD's reanalysis ($3.5 \text{ }^{\circ}\text{C/month}$). In addition, models show a good performance in representing the temporal variation of temperature ($3.5 \leq \text{SD} \leq 5 \text{ }^{\circ}\text{C/month}$).

3.8 SWS

In the SWS (Fig. 8f), most of the models have a moderate correlation ($0.5 \leq \text{CORR} < 0.7$). Two models stand out negatively for the weak or spatial correlation: BCC-ESM1 (0.06) and NorCPM1 (0.03). All models show RMSE values close to the observed SD (20.2 mm/month), except in the case of CAS-ESM2-0 (43.8 mm/month), CNRM-ESM2-1 (45.5 mm/month), IPSL-CM6A-LR-INCA (43.5 mm/month) and MRI-ESM2-0 (46.7 mm/month).

Regarding air temperature (Figure S7f), SWS is where models perform better. Firstly, it is relevant to highlight that the RMSE values $< 1 \text{ }^{\circ}\text{C/month}$ (except for MCM-UA-1-0) are lower than ERA5's SD ($2.5 \text{ }^{\circ}\text{C/month}$). In addition, the models' spatial correlations are robust ($\text{CORR} \geq 0.95$). The SD is also well simulated by models ($2.0 < \text{SD} < 3.5 \text{ }^{\circ}\text{C/month}$).

3.9 SSA

The SSA (Fig. 8g) is the region where models present the better annual standard deviation: the observed SD is 12.4 mm/month, while the models' SD varies between 9.7 and 15.1 mm/month. The SSA is also the region where models show the smaller values of RMSE ($10 < \text{RMSE} < 20 \text{ mm/month}$). Although, it is the region where models show the worst spatial correlation ($0 < \text{CORR} \leq 0.4$).

As well as SES and SWS, models also show a good performance in the simulation of air temperature over SSA (Figure S7g). The observed SD is $2.9 \text{ }^{\circ}\text{C/month}$, and most of the models have SD values between 2.0 and $3.5 \text{ }^{\circ}\text{C/month}$, except CAS-ESM2-0 and MCM-UA-1-0. The model's RMSE values are small, lower than $2.5 \text{ }^{\circ}\text{C/month}$. Regarding the spatial correlation, the values are higher than 0.9, showing a strong correlation.

3.10 Summary of objective analysis

In general, it is clear that models show the lowest correlation in the representation of precipitation in the north (NSA and NWS) and south (SWS and SSA) extremes of SA, where the correlation varies between very weak and weak. Table 3 synthesizes the model's performance over the AR6 regions. The poor performance of models in the NSA and NWS can be associated with the difficulty in simulating the ITCZ, which

Table 3 Summary of the models' performance considering the objective assessment through AR6 regions. Green boxes indicate a good performance, while white boxes indicate a bad performance

CMIP6 Models \ Regions	NSA	NWS	NES	SAM	SES	SWS	SSA
ACCESS-ESM1-5							
AWI-ESM-1-1-LR							
BCC-ESM1							
CanESM5							
CAS-ESM2-0							
CESM2							
CMCC-ESM2							
CNRM-ESM2-1							
E3SM-1-1-ECA							
EC-EARTH3							
FGOALS-f3-L							
FIO-ESM-2-0							
GFDL-ESM4							
GISS-E2-1-G							
HADGEM3-GC31-L1							
IITM-ESM							
INM-CM5-0							
IPSL-CM6A-LR-INCA							
KACE-1-0-G							
MCM-UA-1-0							
MIROC6							
MPI-ESM1-2-HR							
MPI-ESM1-2-HAM							
MRI-ESM-2-0							
NESM3							
NorCPM1							
SAM0-UNICON							
TaiESM1.0							

strongly influences the rainfall pattern in these regions. Regarding the SD representation of the simulated precipitation, models show better performance in dry areas, like SSA. Generally, SAM (SWS) is the region where models deliver the best (worst) implementation in the precipitation simulation. Over SAM, models present an excellent spatial correlation, which can be associated with its well-defined precipitation seasonal cycle. It is worth highlighting the good performance of the EC-EARTH3 model over all AR6 regions.

Regarding the mean air temperature, models show the lowest correlation over northern SA (NSA, NWS, and NES) and over SAM, where the correlation varies between very weak and moderate. Over SA north, the air temperature is directly linked to the precipitation; for this reason, models also show a poor performance in the temperature simulation over these regions. The temperature SD simulated by models performs well over southern SA (SES, SWS, and SSA). Furthermore, CORR values in those regions are upper 0.9 (robust correlation). The main issues about the representation of the precipitation over SES seem to be primarily associated with its magnitude, modulated in the

rainy season mainly due to the flux from north/northwest and requires it to be reasonably well simulated (Barros and Doyle 2018). SWS (NSA) is where models show the best (worst) performance.

Finally, all seven models selected for their best performance in the subjective assessment also show a good and reasonable temperature and precipitation simulation in the objective evaluation.

4 Conclusions and final remarks

This study analyzes the performance of 28 CMIP6 models in representing the present climate (1995–2014) over SA. Some atmospheric variables are spatially evaluated subjectively concerning summer and winter climatologies. From the subjective assessment, the selected seven best models to simulate the climate in SA: ACCESS-ESM1-5, CMCC-ESM2, EC-EARTH3, KACE-1-0-G, MIROC6, MRI-ESM2-0, and TaiESM1-0. An objective evaluation of the precipitation and air temperature series considering each of the 28 models is elaborated for the seven CMIP6 regions in SA. The ensemble formed by the seven best SA models (Top7-CMIP6-SA) is confronted with the ensemble formed by the 28 CMIP6 models (28-CMIP6) used in this research. A spatial evaluation of these two ensembles is elaborated, comparing them with observational and reanalysis data. Finally, both ensembles' temperature and precipitation annual cycles are compared to determine whether working with a preselected ensemble of models (Top7-CMIP6-SA) instead of the whole ensemble (28-CMIP6) would be more advantageous.

The results of the subjective evaluation of spatial patterns of precipitation show that all models perform better in winter (the dry season for most of the South American continent) compared to the rainy season (summer), as already observed in Ortega et al. (2021). All models show a double ITCZ bias in summer and winter, which is common in global climate models. Another common feature of all models is the precipitation underestimation over the NSA and overestimation on the NWS, SWS, and NES during austral summer. The models can reasonably simulate surface variables such as MSLP and air temperature, except for the cold bias simulated over the NES by most of the models. At upper levels, ten models cannot adequately represent the NEB through and BH, resulting in poor simulation of the SACZ. In winter, the ITCZ is better represented by the models compared to summer. In the continental region, the models simulate an excess (deficit) precipitation over the southern SWS (northern NSA and northern NWS). The poor performance of the models in the NSA and NWS may be mainly linked to the difficulty in simulating the positioning of the ITCZ, which strongly impacts the rainfall pattern over these regions. In SSA and SWS, this poor performance may be related to the

misrepresentation of jet streams and the influence of the orography of the Andes Mountains.

In the annual cycle analysis, over SAM and SES, both ensembles (Top7-CMIP6-SA and 28-CMIP6) present a good or satisfactory representation of the annual temperature cycle and precipitation. In the NSA and SES (NES) regions, the Top7-CMIP6-SA ensemble stands out for presenting a superior performance compared to the 28-CMIP6 ensemble regarding the representation of the annual precipitation (temperature) cycle. In austral winter, the Top7-CMIP6-SA ensemble presents the lowest precipitation bias for NSA and SES compared to 28-CMIP6. However, in Austral summer, the performance of the 28-CMIP6 ensemble is superior to the Top7-CMIP6-SA over the SES region.

Regarding the objective temperature and precipitation evaluation, all models in the Top7-CMIP6-SA ensemble present a good or reasonable performance. The results show that the models have the lowest skill in representing precipitation in the extreme northern (NWS and NSA) and SWS regions of SA, according to what was observed in the subjective analysis. The EC-EARTH3 and TaiESM1-0 (MCM-UA-1-0 and NESM3) models present the best (worst) performance in the NES, SAM, and SES regions. In the objective evaluation of the mean air temperature, the models also present a bad performance over NSA and NWS, areas with the lowest spatial correlation values.

Regarding the Top7-CMIP6-SA, these models present a good performance in representing the ITCZ, SJ, and PJ, in addition to the BH and NEB trough, which are characteristic meteorological systems affecting the SA spring and summer. On the other hand, given their poor performance, using the AWI-ESM-1-1-LR, CAS-ESM2-0, IITM-ESM, and NESM3 models is not recommended for studies in SA. These models cannot capture the significant climatological systems influencing SA and show the lowest skill in representing the ITCZ among all 28 models evaluated in this work.

The results found in this study show that the performance of the models depends on the study region, and the models individually cannot reproduce the SA climate, except for the best models included in the Top7-CMIP6-SA. For this reason, the advantage of using an ensemble with the best CMIP6 models only applies to some SA regions, probably due to the climatic diversity of the continent. Future research could employ a more in-depth statistical analysis to identify the nature of the errors and propose a diagnosis. In addition, it is also necessary to verify whether the models that compose the Top7-CMIP6-SA are also able to capture the observed trends in temperature and precipitation extremes observed in the present climate, such as the increasing trends of extreme rainfall events in Southern Brazil (Regoto et al. 2021).

We hope this work can support other scientists who must select CMIP6 models in their research on SA. In this sense,

it is essential to emphasize that although the seven models selected here present good/reasonable performance to represent the prime meteorological systems in the lower and upper levels of the atmosphere, this does not guarantee that they maintain the same performance in the representation of all other variables. Thus, evaluating the climatology of the variable of interest in the reference climate is recommended before using its projections.

Supplementary Information The online version contains supplementary material available at <https://doi.org/10.1007/s00382-023-06979-1>.

Author contributions ACB wrote the article and built the figures, as well as the analysis and discussions of the results. CD and WL-S collaborated with the organization and wrote some of the work's main discussions in addition to revising the article. PR contributed to the methodology development and revised the article.

Funding This research did not receive any specific grant from public, commercial, or not-for-profit funding agencies.

Availability of data The data come from the Copernicus Climate Data Store (CDS), the National Center for Atmospheric Research (NCAR), and the World Climate Research Programme (WCRP). The data are in the public domain and were made available upon request.

Declarations

Conflict of interest The authors declare that they have no known competing financial interests or personal relationships that could have influenced the work reported in this paper.

Ethics approval The authors are committed to upholding the integrity of the scientific record.

Consent for publication All individuals listed as authors have agreed to be listed and approve the submitted version of the manuscript.

References

- Adam O, Schneider T, Brient F (2017) Regional and seasonal variations of the double-ITCZ bias in CMIP5 models. *Climate Dyn* 51(1):101–117. <https://doi.org/10.1007/S00382-017-3909-1>
- Adler RF, Huffman GJ, Chang A, Ferraro R, Xie PP, Janowiak J, Rudolf B et al (2003) The version-2 global precipitation climatology project (GPCP) monthly precipitation analysis (1979–present). *J Hydrometeorol* 4(6):1147–1167. [https://doi.org/10.1175/1525-7541\(2003\)004%3c1147:TVGPCP%3e2.0.CO;2](https://doi.org/10.1175/1525-7541(2003)004%3c1147:TVGPCP%3e2.0.CO;2)
- Almazroui M, Ashfaq M, Islam MN, Rashid IU, Kamil S, Abid MA, O'Brien E et al (2021a) Assessment of CMIP6 performance and projected temperature and precipitation changes over South America. *Earth Syst Environ* 5(2):155–183. <https://doi.org/10.1007/S41748-021-00233-6>
- Alves JMB, Vasconcelos Junior FC, Chaves RR, Silva EM, Servain J, Costa AA, Sombra SS, Barbosa ACB, Dos Santos ACS (2016) Evaluation of the AR4 CMIP3 and the AR5 CMIP5 model and projections for precipitation in Northeast Brazil. *Front Earth Sci* 4(May):44. <https://doi.org/10.3389/FEART.2016.00044/BIBTEX>
- Arias P, Dereczynski C, Alves L, Ruiz-Carrascal D, Rojas M, Sorensson A, Ruiz L et al (2021) Climate change in South America: new insights from the most recent IPCC assessment report. AGU FM
- 2021: GC51B-05. <https://ui.adsabs.harvard.edu/abs/2021AGUFMG51B..05A/abstract>
- Barros VR, Doyle ME (2018) Low-level circulation and precipitation simulated by CMIP5 GCMS over Southeastern South America. *Int J Climatol* 38(15):5476–5490. <https://doi.org/10.1002/JOC.5740>
- Collazo S, Barrucand M, Rusticucci M (2022) Evaluation of CMIP6 models in the representation of observed extreme temperature indices trends in South America. *Clim Change* 172(1):1–21. <https://doi.org/10.1007/S10584-022-03376-1>
- Dias CG, Reboita MS (2021) Assessment of CMIP6 simulations over tropical South America. *Revista Brasileira De Geografia Física* 14(3):1282–1295. <https://doi.org/10.26848/RBGF.V14.3.P1282-1295>
- Garreaud R, Wallace JM (1997) The diurnal march of convective cloudiness over the Americas. *Mon Weather Rev* 125(12):3157–3171. [https://doi.org/10.1175/1520-0493\(1997\)125%3c3157:TDMOCC%3e2.0.CO;2](https://doi.org/10.1175/1520-0493(1997)125%3c3157:TDMOCC%3e2.0.CO;2)
- Hersbach H, Bell B, Berrisford P, Hirahara S, Horányi A, Muñoz-Sabater J, Nicolas J, Peubey C, Radu R, Schepers D, Simmons A, Soci C, Abdalla S, Abellán X, Balsamo G, Bechtold P, Biavati G, Bidlot J, Bonavita M, De Chiara G, Dahlgren P, Dee D, Diamantakis M, Dragani R, Flemming J, Forbes R, Fuentes M, Geer A, Haimberger L, Healy Robin S, Hogan J, Hólm E, Janisková M, Keeley S, Laloyaux P, Lopez P, Lupu C, Radnoti G, de Rosnay P, Rozum I, Vamborg F, Villaume S, Thépaut JN (2020) The ERA5 global reanalysis. *Q J R Meteorol Soc* 146(730):1999–2049. <https://doi.org/10.1002/qj.3803>
- IPCC – Intergovernmental Panel on Climate Change (2021) Climate change 2021: the physical science basis. Contribution of Working Group I to the Fourth Assessment Report on the IPCC. Cambridge University Press, Cambridge
- IPCC – Intergovernmental Panel on Climate Change (2023) Synthesis report of the IPCC sixth assessment report (AR6). Cambridge University Press, Cambridge
- IPCC (2021) Annex II: models [Gutiérrez JM, Tréguier (eds)] In Climate change 2021: the physical science basis. Contribution of working group i to the sixth assessment report of the intergovernmental panel on climate change [Masson-Delmotte V, Zhai P, Pirani A, Connors SL, Péan C, Berger S, Caud N, Chen Y, Goldfarb L, Gomis MI, Huang M, Leitzell K, Lonnoy E, Matthews JBR, Maycock TK, Waterfield T, Yelekçi O, Yu R, Zhou B (eds)]. Cambridge University Press, Cambridge, pp 2087–2138. <https://doi.org/10.1017/9781009157896.016>
- Joetzjer E, Douville H, Delire C, Ciais P (2013) Present-day and future Amazonian precipitation in global climate models: CMIP5 versus CMIP3. *Clim Dyn* 41(11–12):2921–2936. <https://doi.org/10.1007/S00382-012-1644-1/METRICS>
- Kim YH, Min SK, Zhang X, Sillmann J, Sandstad M (2020) Evaluation of the CMIP6 multi-model ensemble for climate extreme indices. *Weather Climate Extremes* 29(September):100269. <https://doi.org/10.1016/J.WACE.2020.100269>
- Monteverde C, De Sales F, Jones C (2022) Evaluation of the CMIP6 performance in simulating precipitation in the Amazon River Basin. *Climate* 10(8):122. <https://doi.org/10.3390/CLI10080122>
- Mukaka M, Moulton L (2016) Comparison of empirical study power in sample size calculation approaches for cluster randomized trials with varying cluster sizes—a continuous outcome endpoint. *Open Access Med Stat* 6:1–7. <https://doi.org/10.2147/OAMS.S96508>
- O'Neill BC, Tebaldi C, Van Vuuren DP, Eyring V, Friedlingstein P, Hurtt G, Knutti R et al (2016) The scenario model intercomparison project (ScenarioMIP) for CMIP6. *Geosci Model Dev* 9(9):3461–3482. <https://doi.org/10.5194/GMD-9-3461-2016>
- Ortega G, Arias PA, Villegas JC, Marquet PA, Nobre P (2021) Present-day and future climate over Central and South America according

- to CMIP5/CMIP6 models. *Int J Climatol* 41(15):6713–6735. <https://doi.org/10.1002/JOC.7221>
- Pabón-Caicedo JD, Arias PA, Carril AF, Espinoza JC, Borrel LF, Goubanova K, Lavado-Casimiro W, Masiokas M, Solman S, Vilalba R (2020) Observed and projected hydroclimate changes in the Andes. *Front Earth Sci* 8(March):61. <https://doi.org/10.3389/FEART.2020.00061/BIBTEX>
- Reboita MS, Gan MA, Rocha RP, Ambrizzi T (2010) Regimes de precipitação na América do Sul: uma revisão bibliográfica. *Rev Bras de Meteorologia* 25(2):185–204. <https://doi.org/10.1590/S0102-7786201000200004>
- Regoto P, Dereczynski C, Chou SC, Bazzanella AC (2021) Observed changes in air temperature and precipitation extremes over Brazil. *Int J Climatol* 41(11):5125–5142. <https://doi.org/10.1002/JOC.7119>
- Ridder NN, Pitman AJ, Ukkola AM (2021) Do CMIP6 climate models simulate global or regional compound events skillfully? *Geophys Res Lett* 48(2):e2020GL091152. <https://doi.org/10.1029/2020GL091152>
- Taylor KE (2001) Summarizing multiple aspects of model performance in a single diagram. *J Geophys Res Atmos* 106(D7):7183–7192. <https://doi.org/10.1029/2000JD900719>
- Taylor KE, Stouffer RJ, Meehl GA (2012) An overview of CMIP5 and the experiment design. *Bull Am Meteorol Soc* 93(4):485–498. <https://doi.org/10.1175/BAMS-D-11-00094.1>
- Tian B, Dong X (2020) The double-ITCZ bias in CMIP3, CMIP5, and CMIP6 models based on annual mean precipitation. *Geophys Res Lett* 47(8):e2020GL087232. <https://doi.org/10.1029/2020GL087232>
- Zazulie N, Rusticucci M, Raga GB (2017) Regional climate of the subtropical central Andes using high-resolution CMIP5 models—part I: past performance (1980–2005). *Clim Dyn* 49:3937–3957. <https://doi.org/10.1007/s00382-017-3560-x>

Publisher's Note Springer Nature remains neutral with regard to jurisdictional claims in published maps and institutional affiliations.

Springer Nature or its licensor (e.g. a society or other partner) holds exclusive rights to this article under a publishing agreement with the author(s) or other rightsholder(s); author self-archiving of the accepted manuscript version of this article is solely governed by the terms of such publishing agreement and applicable law.